7774 *Biochemistry* **2010,** *49,* 7774–7782
DOI: 10.1021/bi100881n

BIOCHEMISTRY
including biophysical chemistry & molecular biology
Article

The Off-Pathway Status of the Alkali Molten Globule Is Unrelated to Heme Misligation and Trans-pH Effects: Experiments with Ferrocytochrome *c*[†]

Abani K. Bhuyan*

School of Chemistry, University of Hyderabad, Hyderabad 500046, India

Received June 1, 2010; Revised Manuscript Received August 4, 2010

ABSTRACT: The relevance of the alkali molten globule (B-state) to the folding pathway of cytochrome *c* has been studied further with the reduced state of the protein for which the B-state is prepared by ligating the ferrous heme iron with extrinsic CO under 1 mM gas concentration in the presence of NaCl. The CO derivative of ferrocytochrome *c* is desirable not only because it abrogates the interference of non-native heme ligands but the GdnHCl-unfolded protein refolds fast without deviating from the intrinsic folding pathway of the protein. Interstate folding−unfolding kinetics at alkaline and neutral pH conditions reveal that the B-state chain initially expands in the submillisecond regime in order to fold correctly to the native state. In this sense, it is an off-pathway nonproductive species which must dissipate some non-native elements before proceeding to fold. It is concluded that the alkali molten globule does not correspond to any possible transient structure in the folding pathway of cytochrome *c*.

Despite being a paradigm for protein folding studies, the oxidized state of horse cyt *c*[1] often offers murky folding scenarios due to solvent and pH-dependent intrapolypeptide−heme misligation. Because of poor affinity of the oxidized heme iron for sulfur-based ligands the Fe^{3+}−M80 bond in ferricyt *c* is weak to begin with. The bond readily ruptures even under mild perturbation of conformation produced by denaturants or alkali, facilitating non-native ligation of the heme iron with other potential intrapolypeptide ligands, histidines and lysines. The chemistry of non-native heme ligation is well understood (*1*−*4*), and a model of ligation kinetics in the context of cyt *c* folding has been proposed earlier (*5*). Briefly, under unfolding conditions at neutral pH, the non-native heme iron−intrapolypeptide contacts, Fe^{3+}−H18 and Fe^{3+}−H26, are so stable that the dissociation rates of these ligands are far smaller than the protein refolding rate (*5*, *6*). As a result, the non-native ligands and parts of the polypeptide they belong to are trapped in the misfolding ensemble. Further folding is rate-limited by the dissociation of the non-native ligands allowing local reconfiguration of the polypeptide chain leading to the native Fe^{3+}−M80 ligation. This later phase of chain reconfiguration coupled with non-native to native ligand swap introduces nonobligatory folding barrier (*7*, *8*). Ferricyt *c* indeed folds fast and downhill when non-native heme ligation is suppressed under appropriate solution conditions (*7*, *8*).

Under extreme alkaline conditions required for producing the B-state, the ligation of the lysyl ε-NH_3^+ groups with the heme iron can compound the heme misligation problem, especially when the pH difference between the initial and final solutions affects the side-chain ionization. The 2 histidines and the 19 lysine residues of the cytochrome polypeptide can generate a large heme ligand-based heterogeneous unfolded ensemble in a pH-dependent manner.

Such ligand interferences could be considered a possible caveat in the companion paper (*9*) where the B-state of ferricytochrome *c* was studied. This study considers ferrocytochrome *c* for which the requirement for molten globule stabilization by itself abolishes the aforementioned ligation-related problems (*10*). Ferrocytochrome *c* at pH 13 binds CO with fairly high affinity ($K_{diss} \sim 22\ \mu M$), and the resultant CO-liganded protein, to be called cyt-CO or carbonmonoxy-cytochrome *c*, can be stabilized into the B-state molten globule by the addition of ∼1 M NaCl (*10*). The binding of extrinsic CO under 1 mM gas concentration obviates the binding of non-native intrapolypeptide ligands and produces a homogeneous population of cyt-CO. In general, GdnHCl-unfolded cyt-CO at pH 7 refolds extremely fast by the same kinetic mechanism that ferrocyt *c* does (*6*, *11*). The heme iron of the refolded molecule still carries the CO at the expense of little conformational perturbation, and slow thermal dissociation of the CO eventually yields to the native M80 ligation. In summary, refolding of cyt-CO encounters no ligand interference and the kinetics are relatively unambiguous.

With this background the present study uses the B-state of ferrocytochrome *c* (also called ferrocyt B-state) to further examine the relevance of the steady-state alkali molten globule in the kinetic pathway of cytochrome *c* folding.

MATERIALS AND METHODS

Since the strategy and approaches to experiments here were virtually identical to those described in the preceding paper (*9*), the details of buffer systems, solvent conditions, protein preparation,

[†]Funds for this research were provided by Grants BRB/15/227/2001 and BRB/10/622/2008 from the Department of Biotechnology, Government of India.

*To whom correspondence should be addressed. E-mail: akbsc@uohyd.ernet.in. Phone: 91-40-2313-4810. Fax: 91-40-2301-2460.

[1]Abbreviations: GdnHCl, guanidine hydrochloride; cyt *c*, cytochrome *c*; ferricyt *c*, ferricytochrome *c*; ferrocyt *c*, ferrocytochrome *c*; cyt-CO, carbon monoxide-bound ferrocytochrome *c*; alkaline cyt-CO, alkali-unfolded cyt-CO; MG, molten globule; $\Delta G_D°$, Gibbs energy of denaturation in the absence of denaturant; m_g, protein surface area associated with denaturant unfolding transition; B-state or ferrocyt B-state, alkali molten globule of ferrocyt *c* where the heme iron is ligated to CO; N, native state at pH 7; N_B, N-state of cyt-CO at alkaline pH; U, unfolded state at pH 7; U_B, alkali-unfolded state of cyt-CO with or without GdnHCl; PFG NMR, pulsed-field-gradient NMR.

 Published on Web 08/05/2010

and instrumentation are omitted. However, cytochrome *c* for all experiments described here was essentially and strictly maintained in the reduced form liganded with CO. The general procedure for generating carbonmonoxy-cytochrome *c* (cyt-CO) involved exhaustive deaeration of the protein solution by blowing argon or nitrogen over the sample contained in a cuvette or NMR tube set to rock, reduction of the heme iron by the addition of a freshly prepared concentrated solution of $Na_2S_2O_4$, addition of dry CO by gently bubbling the gas into the solution for a minute, and tight capping of the sample cell by the use of an appropriate sleeved stopper. The procedure, applied consistently to each sample, did not upset the pH and the protein concentration appreciably. The final concentration of $Na_2S_2O_4$ was 2−3 mM for steady-state and stopped-flow fluorescence experiments and 12−15 mM for NMR spectra. The CO concentration was 1 mM. For stopped-flow experiments, the procedure of sample reduction and CO ligation was carried out with protein and refolding/unfolding buffer solutions contained in gastight Hamilton syringes. Since heme autoxidation is relatively reduced at higher pH, the cyt-CO samples thus prepared are stable for at least 24 h even in the presence of high concentrations of GdnHCl.

RESULTS

Formation and Stability of the Ferrocyt B-State. Horse ferrocyt *c* as such is energetically so stable that it barely unfolds even at the extreme of amenable alkaline pH (*12*). However, the heme iron of the destabilized protein readily binds extrinsically added CO with an apparent association constant $K_{assoc} \sim 45.4$ mM^{-1} at pH 13. The CO binding process, essentially a replacement of the preexisting Fe^{2+}−M80 bond, liberates the M80-resident part of the polypeptide, causing the molecule to expand and denature. The denatured CO-bound alkaline ferrocytochrome *c* (cyt-CO) is called the U_B-state. Figure 1a recapitulates the fluorescence-monitored formation of the U_B-state at basic pH in the presence of 1 mM CO. The characteristic of the transition, three OH^- titration with a pH midpoint of 12.6, is quite similar to the alkaline transition of ferricyt *c* observed in the accompanying paper (*9*). Figure 1b shows the NaCl-driven $U_B \rightarrow B$ transformation at pH 13 featured by binding of one or two Na^+ with a transition midpoint $C_m \sim 0.05$ M NaCl. A comparison with the corresponding transition for ferricyt *c* described in the preceding paper (*9*) would show that the $U_B \rightarrow B$ transition for both oxidation states of cyt *c* involves binding of one or two Na^+; however, the C_m value for the ferrocyt $U_B \rightarrow B$ transition is half the value for the ferricyt case, suggesting higher stability of the former. As extracted from the GdnHCl melt (Figure 1c and Table 1), the $\Delta G°$ value for the ferrocyt B-state is 4.05 (±0.6) kcal mol^{-1}, which is 2-fold larger than the value for ferricyt B-state.

Since the ferrocyt B-state has already been tested for the generic molten globule criteria (*10*), the basic spectroscopic data are not reproduced here. To supplement the earlier report, the hydrodynamic radii (R_H) of the B-state and all other related states of cyt-CO were determined by PFG NMR diffusion measurement as represented in Figure 1d for the B- and N_B-states. Values of R_H listed in Table 2 suggest that the alkaline native state (N_B), even though considered native because of its quenched fluorescence, is considerably expanded relative to the native state at pH 7 (N). It is also noticed that the binding of CO to the reduced heme leads to further molecular expansion. As discussed above, the Fe^{2+}−M80 → Fe^{2+}−CO replacement causes the M80-containing part of the polypeptide to move away from the heme proximity facilitating chain opening.

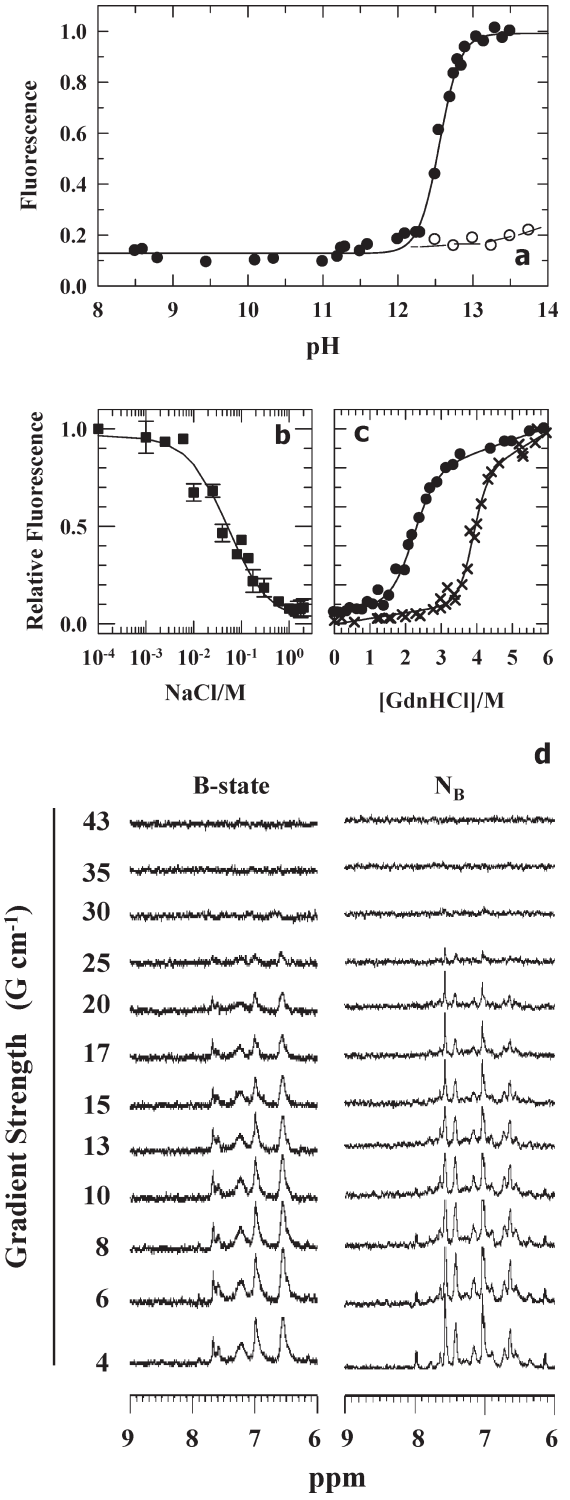

FIGURE 1: (a) Alkaline pH unfolding of cyt-CO (●). The transition is characterized by a pH midpoint of 12.55 and titration of three OH^-. The open circles show quenched fluorescence for ferrocyt *c* samples that did not contain CO. (b) The NaCl-induced transformation of cyt-CO to the B-state at pH 13. The fluorescence of the molten globule is as quenched as that of the native protein. (c) GdnHCl-induced unfolding transitions for the B-state at pH 13, 1 M NaCl (●), and the N-state at pH 7, 0.1 M phosphate buffer (×). The two-state fit parameters for these transitions are listed in Table 1. (d) Representative PFG NMR spectra of the B-state and native ferrocyt *c* at pH 13 in the absence of CO (also called the N_B-state). Values of R_H extracted from these experiments are listed in Table 2.

Folding of the B-State at Alkaline pH. In this experiment the B-state prepared in 1 M NaCl at pH 12.9 was allowed to

Table 1: Values of $\Delta G°$ (kcal mol^{-1}) and m_g (kcal mol^{-1} M^{-1}) for Fluorescence-Monitored GdnHCl Unfolding of N- and B-States at 22 (±1) °C[a]

		equilibrium		kinetic	
transition	condition	$\Delta G°$	m_g	$\Delta G°$	m_g
N ⇌ U	0.1 M phosphate, pH 7	11.0 (±0.7)	2.8 (±0.2)	10.2 (±1.4)	2.8[b]
B ⇌ U_B	water−NaOH, pH 13	4.0 (±0.6)	1.8 (±0.2)	4.6 (±0.8)	2.0 (±0.4)
N_B ⇌ U_B	water−NaOH, pH 11.5	2.1 (±0.4)	1.0 (±0.2)	1.5 (±0.4)	0.7 (±0.2)

[a]The heme iron is always liganded with CO. [b]Constrained fit.

Table 2: Hydrodynamic Radii (R_H) of Various States Related to the Ferrocyt B-State at 22 (±1) °C

state	condition	R_H (Å)
N (native, −CO)	0.1 M phosphate, pH 7	17.9 (±1.5)
N_B (alkaline native state, −CO)	water−NaOH, pH 13.0	20.7 (±1.9)
U_B (alkali denatured, +CO)	D_2O−NaOD, pH 13.2	23.9 (±1.7)
U_B (alkali denatured, +CO, +4.3 M GdnHCl)	D_2O−NaOD, pH 12.9	23.1 (±1.5)
B (alkali molten globule, +CO)	water−NaOH, 2 M NaCl, pH 13.1	22.8 (±1.2)

refold by stopped-flow dilution with a CAPS buffer containing 0.75 M NaCl and variable amounts of GdnHCl held at pH 9. The pH of the mixed solution was in the 11.7−12.0 range. Under these conditions the protein refolds to the alkaline native state (N_B) while the differences in pH and ionic strength between the initial and final solutions are not substantial. The traces plotted in Figure 2a,b show that a burst increase of fluorescence is followed by two relaxation processes. The GdnHCl dependences of the observed rate constants (λ's) produce two distinct nonoverlapping chevrons (Figure 2c), indicating the formation of an intermediate "I", the fractional amplitude of which is shown in Figure 2d. However, both chevrons feature rollover at both ends, which, according to the general interpretation, is indicative of the existence of additional transient intermediate(s) by which "I" is formed and dissipated. The negative slope of the folding limb for both chevrons is suggestive of misfolded nature of these intermediates. Aggregation during folding is unlikely because the magnitude of the negative slope appeared constant with varying protein concentration (results not shown). Evidently, the kinetics are complex, and the details of GdnHCl dependence of λ's is not analyzed here. The increase of burst fluorescence as a function of GdnHCl concentration (Figure 2e) suggests a substantial expansion of the B-state chain as soon as it is placed in the refolding medium. The expanded burst product B′ need not structurally or energetically resemble the U_B-state. To account for the multitude of intermediates, the major events in the folding of the B-state under alkaline conditions can be qualitatively schematized as shown in Scheme 1.

These kinetics are similar to those observed for ferricyt B-state folding at alkaline pH (*9*). The molten globule must first unfold in order to reconfigure the chain toward the formation of a kinetic intermediate, I. The abortive nature and hence the lack of direct accessibility to the native state should imply that the B-state is redundant for protein folding.

Folding of the U_B-State at Alkaline pH. The observation above that the kinetics of B-state folding is atypical of a molten globule-like intermediate led to examine the folding of the U_B-state under alkaline conditions. Here, the U_B-state prepared in 4 M GdnHCl and 0.75 M NaCl, pH 12.7, was mixed with 30 mM CAPS buffer containing 0.75 M NaCl and variable amounts of GdnHCl. The final pH of the mixture was measured in the 11.7−12.0 range. The traces in Figure 3a show a burst decrease of fluorescence signal which decreases further in the millisecond regime by a discrete phase. In addition to these two phases of fluorescence quenching common to all traces, a slow phase by which the fluorescence changes in a GdnHCl-dependent manner is also observed. The GdnHCl dependences of the two observable rate constants (Figure 3b) and the corresponding fractional amplitudes (Figure 3c) are similar to those seen earlier in the case of B-state folding (see Figure 2), and suggest the involvement of a compact millisecond intermediate which is formed and dissipated through additional intermediate(s). The GdnHCl dependence of the signal at $t = 0$ and $t = \infty$ along with the steady-state fluorescence measured by an independent equilibrium melt at pH 11.7 (Figure 3d and Table 1) indicates that the burst product unfolding transition roughly simulates the transition for the N_B-state (N_B ⇌ U_B). These observations suggest that the burst fluorescence product formed in the folding reaction of U_B is represented by a collapsed chain which undergoes further compaction into a millisecond kinetic intermediate. A minimal mechanism consistent with these observations is shown in Scheme 2, where U_B' is the collapsed burst product and "I" represents the intermediates. Whether to call U_B' an early intermediate or not is debatable (*8*, *13*−*17*), especially in the dearth of detailed data at hand. The mechanisms depicted in Schemes 1 and 2 are different mainly with respect to the nature of the initial burst product: U_B' is a contracted state with quenched fluorescence and B′ is an expanded state highly fluorescent (see Figures 2a,b and 3a).

Kinetics of the B ⇌ U_B Equilibrium. The existence of this equilibrium has been discussed already in the context of the stability of the B-state (Figure 1c and Table 1). Now, the occurrence of B′ and U_B', the former expanded and the latter contracted, in the folding pathways of B- and U_B-states is intriguing. Therefore, the kinetics of folding−unfolding of the B-state were studied in a series of experiments where the U_B-state (cyt-CO in 3.6 M GdnHCl, 1 M NaCl, pH 12.9) and the B-state (cyt-CO in 1 M NaCl, pH 12.9) were allowed to fold and unfold, respectively, by stopped-flow dilution into an aqueous solution of 1 M NaCl at pH 12.8 containing variable amounts of GdnHCl. The traces for the refolding of U_B (Figure 4a) are characterized by a burst fluorescence quench followed by three exponentially decaying phases. The traces for the unfolding of the B-state (Figure 4b), on the other hand, register a burst fluorescence increase followed by a fast phase of fluorescence decay and an intermediate and a slow phase of fluorescence rise. The GdnHCl dependences of the

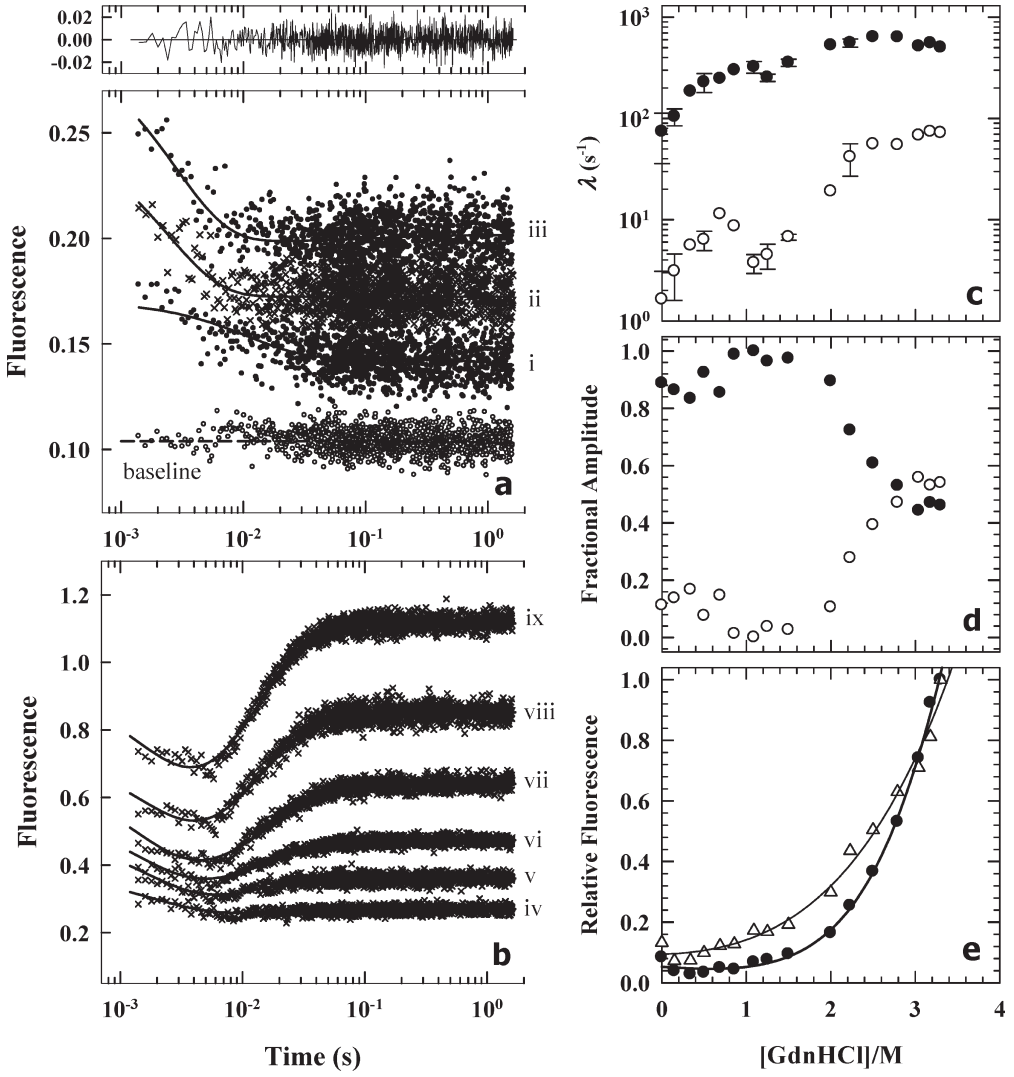

FIGURE 2: Kinetics of the B ⇌ N_B process at alkaline pH. (a) The traces for the folding of the B-state (pH 12.9) to the N_B-state (pH 12) are characterized by a burst fluorescence increase followed by a major and a minor phase of fluorescence decrease. GdnHCl concentrations in the refolding medium are (i) 0.15 M, (ii) 1.1 M, and (iii) 1.5 M. (b) In unfolding, the burst product first quenches by a minor amplitude fast phase which is followed by the major phase of fluorescence increase associated with protein unfolding. GdnHCl concentrations specific to the displayed traces are (iv) 2.0 M, (v) 2.3 M, (vi) 2.5 M, (vii) 2.8 M, (viii) 3.0 M, and (ix) 3.3 M. (c) Chevron plots for the two observable phases, fast (●) and slow (○). The inflection point for both chevrons is centered at 1 (±0.1) M GdnHCl. Error bars were calculated from either iterative fits at different stages of averaging of a single set of data points averaging or two independently recorded data sets. (d) GdnHCl dependence of fractional amplitudes of the two observable phases indicates association of the fast (●) and slow (○) phases with folding and unfolding, respectively. (e) GdnHCl dependence of fluorescence at $t = 0$ (Δ) and $t = \infty$ (●).

Scheme 1

$$B \longrightarrow B' \rightleftharpoons \left[\cdots I_j \cdots\right] \rightleftharpoons I \rightleftharpoons \left[\cdots I_k \cdots\right] \rightleftharpoons N_B \rightleftharpoons \left[\cdots I_l \cdots\right] \rightleftharpoons U_B$$

Scheme 2

$$U_B \longrightarrow U_B' \rightleftharpoons \left[\cdots I_j \cdots\right] \rightleftharpoons I \rightleftharpoons \left[\cdots I_k \cdots\right] \rightleftharpoons N_B \rightleftharpoons \left[\cdots I_l \cdots\right] \rightleftharpoons U_B$$

observable rates (λ_i, $i = 1, 2, 3$) produce three distinct chevrons with minima at ~1.2 M GdnHCl for λ_1 and λ_2 and ~2.1 M GdnHCl for λ_3 (Figure 4c). The denaturant dependences of fractional amplitudes corresponding to the λ's (Figure 4d) suggest that the fast phase (λ_1) is related to the formation of a kinetic intermediate that populates maximally around 1.2 M GdnHCl. At this denaturant concentration, the amplitude corresponding to λ_2 is at the lowest, but it gains as the transition region is approached and accounts for half of the total observable amplitude at the transition midpoint. The slow phase (λ_3) whose amplitude is always within 20% may originate from a minor population of U_B molecules following a parallel pathway. In the unfolding kinetics where the B-state is driven to unfold to U_B, this slow phase is dominating near the transition midpoint but diminishes strongly at higher denaturant concentrations. The unfolding kinetics is also characterized by a burst phase of fluorescence increase (Figure 4b,e), meaning an initial B-state expansion, followed by a fast phase (λ_1) of fluorescence decrease which translates to a chain contraction and an intermediate phase (λ_2) of unfolding. The fractional amplitudes for λ_1 and λ_2 as a

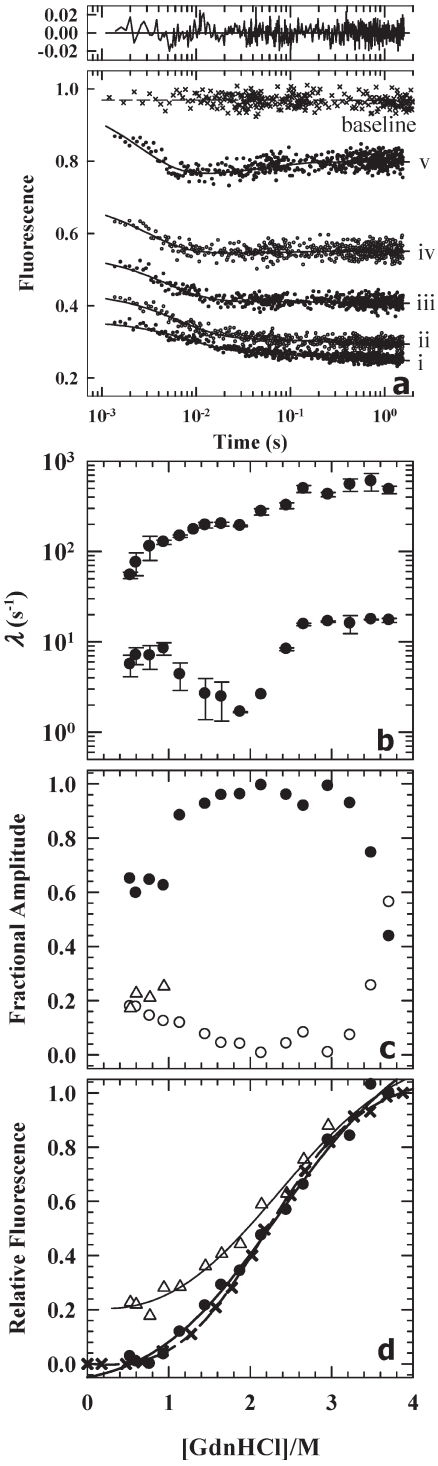

FIGURE 3: Kinetics of the $U_B \rightleftharpoons N_B$ equilibrium at alkaline pH. (a) The U_B protein prepared at pH 12.7, 4 M GdnHCl is highly fluorescent (baseline). Upon dilution into a pH 12.0 buffer, the protein refolds to the N_B-state by an initial burst fluorescence quench followed by two decaying exponentials. The GdnHCl concentrations specific to these traces are (i) 0.8 M, (ii) 1.1 M, (iii) 1.7 M, (iv) 2.5 M, and (v) 3.7 M. (b) The chevrons for the two observable phases, fast (●) and slow (○), show an inflection centered at ~1.9 M GdnHCl. Error bars were calculated as described for Figure 2c. (c) The fractional amplitudes for the two observable phases, fast (●) and slow (○). (d) GdnHCl dependence of the normalized fluorescence signal at $t = 0$ (Δ) and $t = \infty$ (●). The latter reproduces the equilibrium unfolding transition determined independently at pH 12.0 (×).

function of GdnHCl increase in parallel (Figure 4d), indicating the possibility of two parallel unfolding pathways.

The results suggest that the kinetic mechanism of the $B \rightleftharpoons U_B$ process is simply not concerned with Na^+-mediated electrostatic shielding but also involves ultrafast processes and millisecond intermediates occurring in parallel pathways.

Folding Kinetics of B- and U_B-States at Neutral pH. The rationale for this experiment, where the B-state (2 M NaCl, pH 12.9) and the U_B-state (1 M NaCl, pH 12.9, with or without 4 M GdnHCl) were allowed to fold at pH 7 as a function of GdnHCl, is that the folding speed of the B-state will be radically faster than that for the U_B-state if the former is the prototype of a native-like kinetic intermediate. However, earlier double-jump stopped-flow studies in conjunction with hydrogen-exchange pulse labeling NMR measurements showed that the alkali-unfolded cyt-CO or the U_B-state misfolds extensively when placed under native-like conditions at pH 7 (*18*). In spite of misfolding, the simplicity of the overall kinetic mechanism for the folding of the U_B-state at pH 7 should allow for a comparison with the kinetic behavior of the B-state under identical refolding conditions.

Figure 5 shows some details of B-state folding kinetics. There is a burst signal change which could not be quantified due to the nature of the quenched fluorescence of the initial B-state at alkaline pH relative to the fluorescence after dilution at pH 7. At low concentrations of GdnHCl (< 2 M), two exponential phases are required to fit the data, a fast phase characterized by increase of fluorescence and a very slow minor-amplitude phase, which disappears at higher denaturant concentration, associated with fluorescence decrease (Figure 5a). The minor will be not considered further. At still higher denaturant concentration, the protein unfolds by a single phase of fluorescence increase (Figure 5b). The interesting feature of the rate-denaturant profile (Figure 5c) is an accentuated rollover of the folding limb with a positive slope nearly equaling the slope of the unfolding limb. This is typical of refolding kinetics of alkaline cyt-CO studied earlier where an abortive mechanism involving a dead-end intermediate was established (*18*). The inverted chevron in Figure 5c has been fitted with one of the observable eigenvalues (λ_2) obtained from numeric solution of Scheme 3. The variations of the four microscopic rate constants (k_i, i = IU, UI, UN, NU) in the GdnHCl range employed are also obtained from the simulation (Figure 5d and Table 3). The position of the chevron minimum along the denaturant axis and the GdnHCl dependence of the $t = \infty$ signal (Figure 5e) indicate that the folding kinetics recorded here are atypical of a native-like kinetic intermediate but rather are characteristic of an unfolded species. Hence, the B-state is not a model for a late kinetic intermediate.

Scheme 3

$$B \dashrightarrow I \rightleftharpoons U \rightleftharpoons N$$

Table 3: Numeric Calculations of the $I \rightleftharpoons U \rightleftharpoons N$ Model for Refolding of B- and U_B-States at pH 7[a]

	numeric value (in water, s^{-1})	
microscopic rate constant	B-state	U_B-state
k_{UI}	5250	5250 (±1729)
k_{IU}	36	40 (±13)
k_{UN}	23200	6590 (±2040)
k_{NU}	0.012	0.0015 (±0.0005)

[a]Error range for corresponding k_i values of B- and U_B-states is similar.

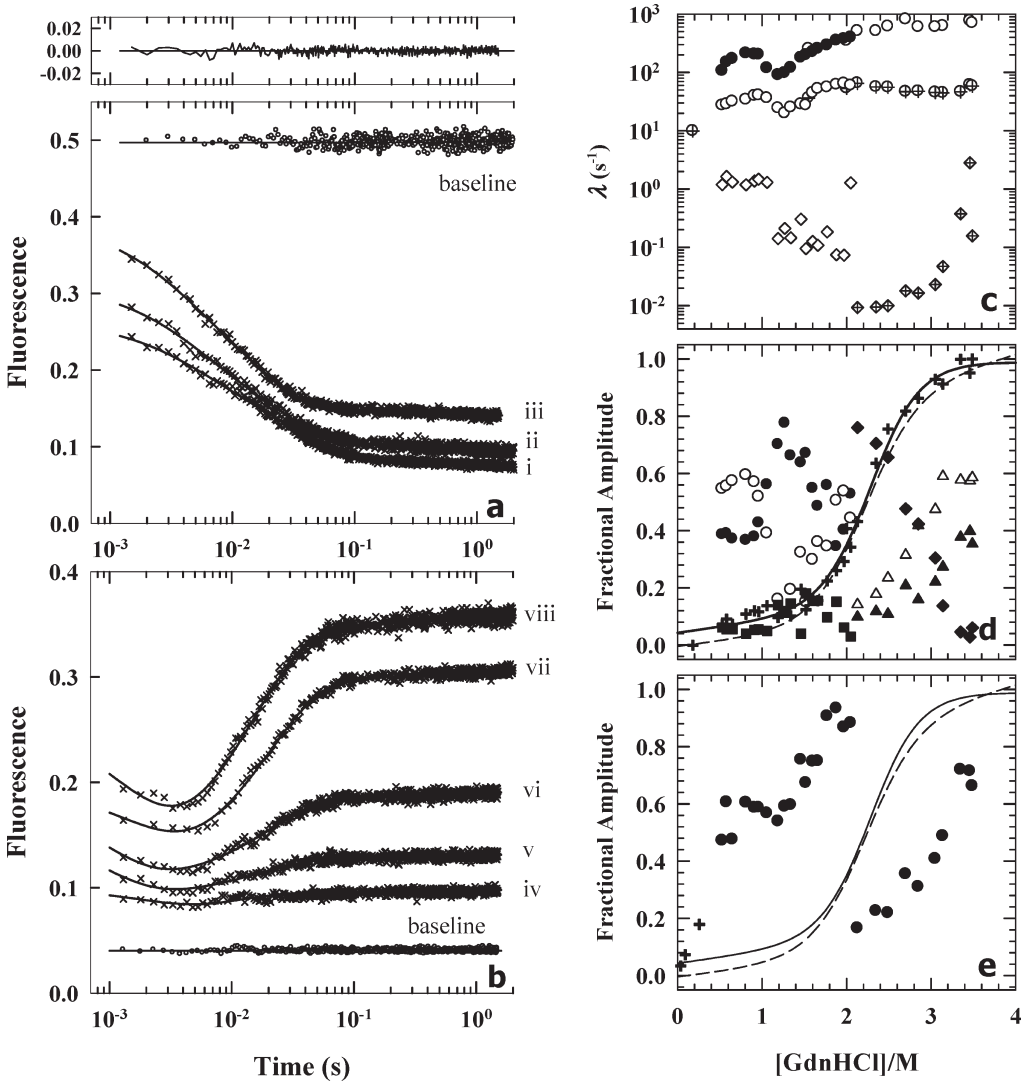

FIGURE 4: Kinetics of the $U_B \rightleftharpoons B$ equilibrium where folding to the molten globule is allowed from the U_B-state prepared initially in 3.6 M GdnHCl, pH 12.9. (a) The folding traces are described by a burst fluorescence decay followed by three exponentials of fluorescence quench. The trace labels i, ii, and iii correspond to 0.7, 1.0, and 1.5 M GdnHCl, respectively. (b) Unfolding of the B-state also occurs by a burst signal increase followed by a fast exponential decay and two slower phases of growing exponentials. The GdnHCl concentrations corresponding to traces iv−viii are 2.0, 2.4, 2.7, 3.1, and 3.5 M in the increasing order of the label. (c) GdnHCl dependence of observed rate for the fast (●), intermediate (○), and slow (◇) phases. (d) Fractional amplitudes, fast (● and ▲), intermediate (○ and △), and slow (■ and ♦), $t = \infty$ fluorescence (+ and solid line), and the equilibrium unfolding transition (dashed line) reproduced from Figure 1c. The fit parameters are given in Table 1. (e) GdnHCl dependence of the burst fluorescence normalized with respect to the fluorescence of the initial state of the protein. Both folding and unfolding kinetics register burst signal change.

To provide a reference kinetic scenario for comparison with the B-state folding, the refolding data for 4 M GdnHCl-unfolded alkaline cyt-CO (the U_B-state) are presented in Figure 6. The highly fluorescent baseline generated by the U_B protein facilitates quantification of the burst phase (Figure 6a). Of the two observable folding phases the minor-amplitude (~10%) slow phase was discarded from further analysis. Clearly, the chevron features are very similar to what is observed for the B-state (Figure 5c). It is noted that exclusion of GdnHCl from the initial preparation of alkaline cyt-CO produces no considerable differences in the folding kinetics (see Figure 6b). Here also, the rate-denaturant behavior was modeled with the dead-end mechanism (Scheme 3), and numerically simulated variations of λ_2 and k_i with GdnHCl are shown in Figure 6b,c. As reported earlier (*18*), the abortive intermediate (I in Scheme 3) is likely to form in the folding burst phase (Figure 6d).

To summarize the main results, Figure 7 compares the relevant folding chevrons. The folding mechanisms for B- and U_B-states are very similar under both alkaline (Figure 7a) and neutral pH conditions (Figure 7b). While the horizontal chevron shifts observed under alkaline conditions arise from disparate stabilities of B- and N_B-states, the vertical shifts under both conditions are due to differences in the compactness and hence differential requirement of chain diffusion to achieve the rate-determining transition state. In spite of these differences, the same overall folding mechanism is shared by the molten globule and the unfolded state. It is thus concluded that the alkali molten globule studied here is not a model for a kinetic intermediate.

DISCUSSION

The Alkali Molten Globule of Cytochrome c Is an Off-Pathway Species. But for the possibilities of interference of non-native heme ligands and some trans-pH effects on the folding under alkaline conditions, the study presented in the accompanying paper (*9*) has already concluded that the B-state does not model a kinetic intermediate, not a late intermediate, at

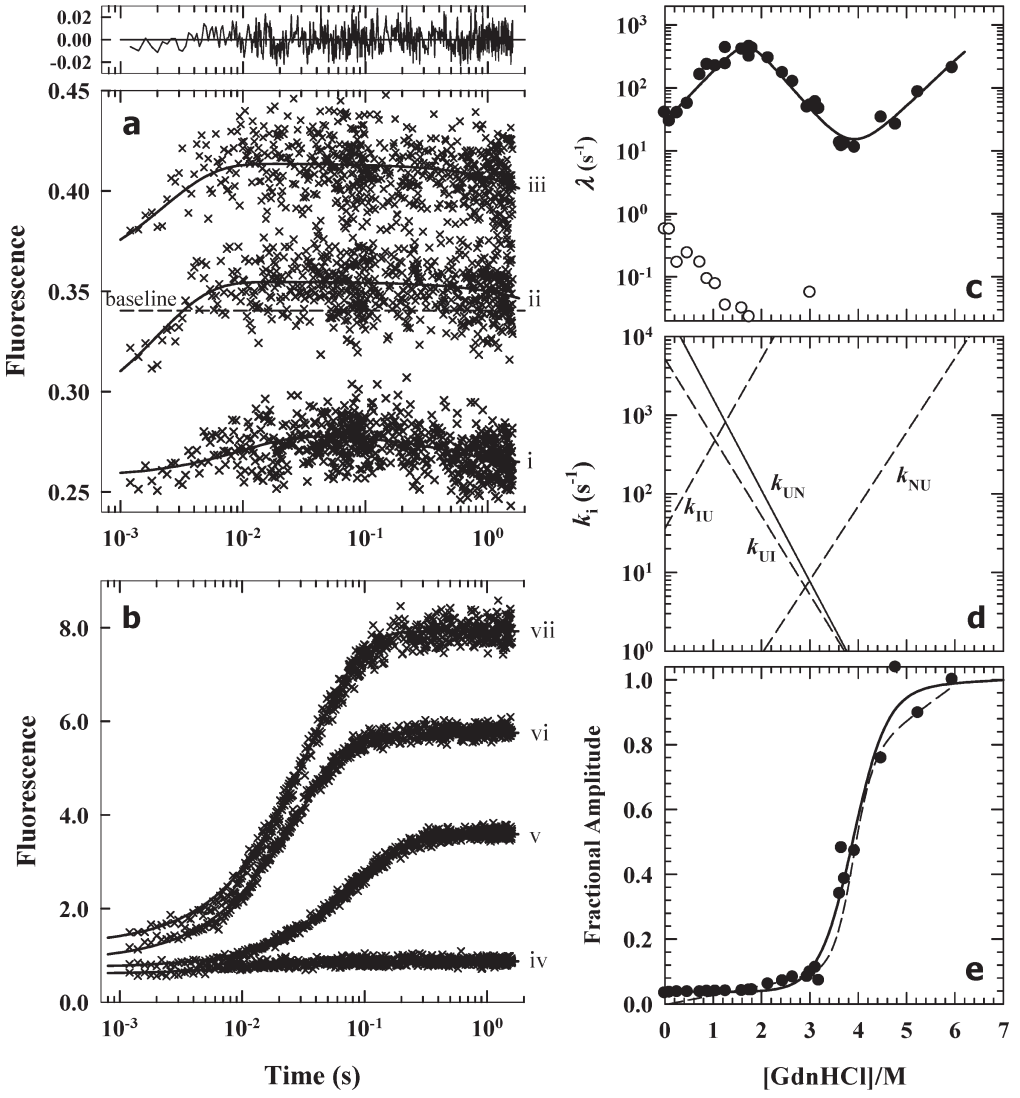

FIGURE 5: Refolding of the B-state (pH 12.9, 2 M NaCl) at a final pH 7. (a) Two-exponential fits of refolding traces at 0.1, 1.3, and 1.7 M GdnHCl, labeled as i, ii, and iii, respectively. (b) Single-exponential unfolding kinetics in the presence of 3.1, 3.9, 4.5, and 4.8 M GdnHCl labeled from iv to vii in the increasing order. (c) Inversion of the chevron under strongly native-like conditions is an indication of the occurrence of an off-pathway intermediate. The solid line through the data is the simulated λ_2 for the off-pathway B $\rightarrow$ I $\rightleftharpoons$ U $\rightleftharpoons$ N mechanism as described in the text. The irreversible B $\rightarrow$ I segment was excluded from simulation. The fit for λ_1 is out of scale in the graph. (d) Denaturant dependences of the microscopic rate constants, k_{IU}, k_{UI}, k_{UN}, and k_{NU}, for the I $\rightleftharpoons$ U $\rightleftharpoons$ N mechanism. (e) The $t = \infty$ fluorescence signal extracted from the kinetic traces reproduces the equilibrium unfolding transition of cyt-CO at pH 7 (see Figure 1c).

least. In the present study, these two possibilities were largely suppressed by using the CO-bound ferrocyt *c* poised across the initial and final conditions in a way that minimized the influence of pH-dependent electrostatic effects. The kinetics still are far from simple. The argument here is that if the molten globule is a steady-state model of a postbarrier late kinetic intermediate (*7*, *19*−*24*), then the B-state molecule should have refolded extremely fast without populating kinetic intermediates just as expected for a downhill folding scenario. Instead, the observed kinetics are slow and barrier-limited, and the possible folding mechanisms require invocation of kinetic intermediates. Since these kinetic features are also detected in the refolding of the GdnHCl-unfolded protein irrespective of the initial pH and in both oxidation states of the heme, it is tempting to conclude at least in terms of the kinetic criteria that the alkali molten globule resembles the unfolded protein rather than being an analogue of transient folding intermediates. There is hard evidence, however, that the B-state of cytochrome *c* is a highly qualified ordered molten globule (*10*, *25*), meaning that it must be structurally and conformationally distinct from the denaturant-unfolded protein. The apparent difficulty as to how a compact native-like protein could kinetically resemble the unfolded state is resolved by the results presented. For all refolding experiments conducted in both redox states of cytochrome *c*, the B-state has been invariably found to exhibit an initial phase of molecular expansion. This event should therefore produce a state that would structurally resemble the denaturant-unfolded state. It can then be said that the B-state has to unfold first in order to access the native state, and hence it is an off-pathway species.

Misfolding or abortive nature of some molten globules has become known in very recent studies. For example, non-native docking of helices in the equilibrium molten globule of *Azotobacter* apoflavodoxin seems to prevent the formation of the native state (*26*, *27*). In certain variants of human carbonic anhydrase II, the molten globule light intermediate that appears during equilibrium unfolding transition becomes trapped in a misfolded state (*28*). For apomyoglobin, the ensemble of the rapidly formed molten globule-like kinetic intermediate has been

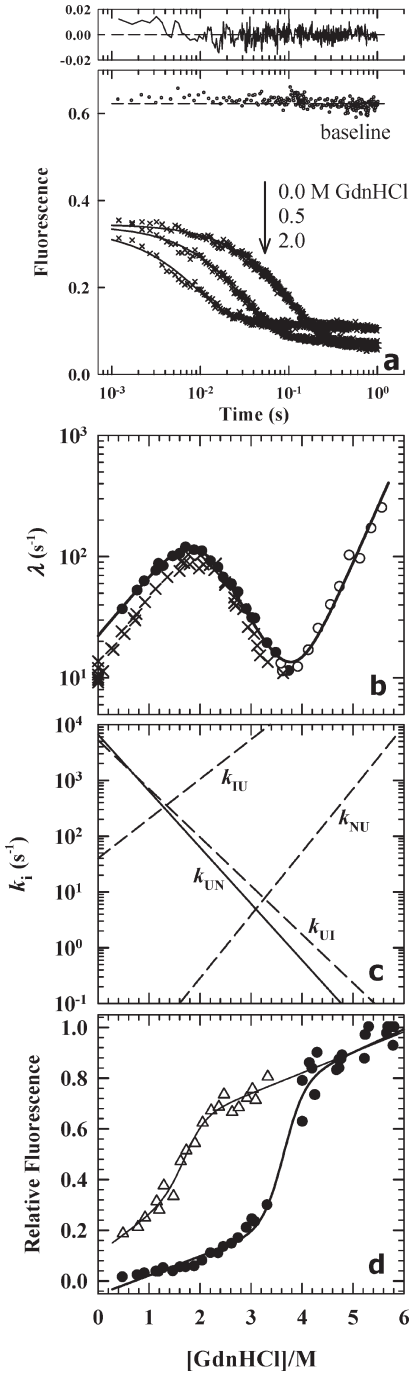

FIGURE 6: Kinetics of refolding from the U_B-state (pH 12.9, 1 M NaCl, with or without 4 M GdnHCl) to the N-state at pH 7. (a) Following the burst decrease of fluorescence, two exponentials are needed to fit the refolding traces, where the slow phase accounts for 8−17% of the total observable amplitude. The residual shown is for refolding to 0 M GdnHCl. (b) The observed relaxation rate constant as a function of final GdnHCl for two independent experiments depending upon whether the initial U_B-state preparation contained 4 M GdnHCl and 1 M NaCl (●) or not (×). The solid line represents the calculated behavior of λ_2 as a function of GdnHCl for the B → I ⇌ U ⇌ N mechanism. The B → I segment was excluded for rate calculations. (c) Dependences of the microscopic rate constants k_{IU}, k_{UI}, k_{UN}, and k_{NU} on GdnHCl. (d) GdnHCl dependences of $t = 0$ and $t = \infty$ fluorescence obtained from kinetic traces represent the transitions for the off-pathway intermediate that accumulates in the burst phase and the equilibrium unfolding transition of cyt-CO at pH 7 as shown in Figure 1c. Values of $\Delta G°$ and m_g estimated from the fit to the burst signal data are 4.8 kcal mol^{-1} and 2.8 (constrained) kcal mol^{-1} M^{-1}. Values for two-state fit parameters for the $t = \infty$ signal are listed in Table 1.

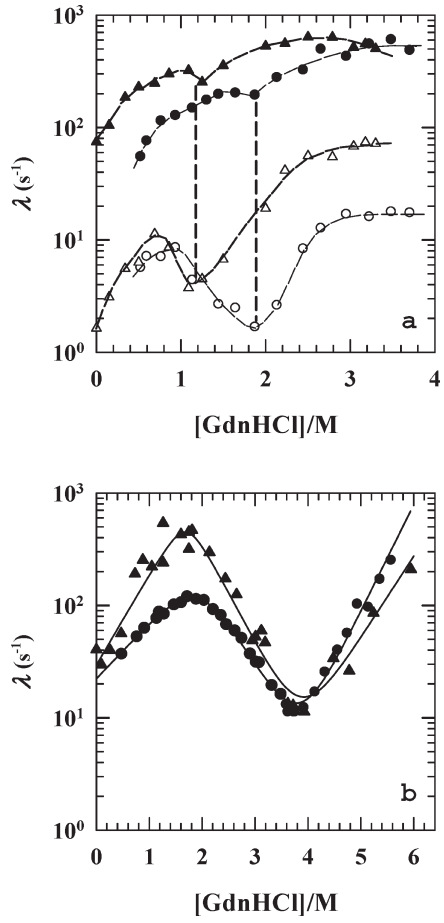

FIGURE 7: Comparison of chevrons for the folding of the B-state and the GdnHCl-unfolded U_B-state. (a) At pH 12.9, B-state (▲ and ▲, fast and slow phases, respectively) and U_B-state (● and ●, fast and slow phases, respectively). Lines through data points are drawn by inspection only. The broken vertical lines connect the inflection points of chevrons. (b) At pH 7, B-state (▲) and U_B-state (●).

found to contain molecules where helix docking is topologically correct, but some non-native local interactions persist (*29*) which must be dissipated for these structures to fold correctly. The equilibrium B-state of cytochrome *c* is speculated to belong to such class of structures where the organization of the secondary structural elements are topologically native-like, but they harbor non-native local interactions, the dissolution of which may register as the burst unfolding phase. A test for this will require residue-level characterization of the B-state.

Caution Concerning the Structure and Role of Molten Globules. The study presented here does not attempt to discard the idea that steady-state molten globules may be structurally similar to transient kinetic intermediates. The idea must be considered a hypothesis that needs to be tested. As already discussed, the correlation seems to hold for some proteins. For ferricytochrome *c*, earlier studies have found that in pH 2 → pH 4.9 or 6.2 jumps, the refolding time constant for the A-state of ferricyt *c* (pH 2, NaCl) is at least 15-fold larger than that for the GdnHCl-unfolded protein initially held at pH 2 (*7*), which subscribes to the view that the acid molten globule models a near-native state appearing beyond the rate-limiting barrier. The inconsistent results presented with the basic molten globule here as well as in other studies surveyed above ask for two cautions. One, the equilibrium molten globule need not necessarily be structurally similar to the kinetic molten globule. The structural similarity

should be investigated in a protein-specific manner with due regard to the solvent conditions used to stabilize the molten globules. Also, residue-specific characterization of the molten globules rather than relying on their global parameters is desirable (*30*). Two, the molten globule, either or both of equilibrium and kinetic forms, can carry non-native interactions to variable extents, in which case they are off-pathway species and their relevance to protein folding is uncertain.

REFERENCES

1. Muthukrishnan, K., and Nall, B. T. (1991) Effective concentrations of amino acid side chains in an unfolded protein. *Biochemistry 30*, 4706–4710.
2. Elöve, G. A., Bhuyan, A. K., and Roder, H. (1994) Kinetic mechanism of cytochrome *c* folding: involvement of the heme and its ligands. *Biochemistry 33*, 6925–6935.
3. Pierce, M. M., and Nall, B. T. (1997) Fast folding of cytochrome *c*. *Protein Sci. 6*, 618–627.
4. Colón, W., Wakem, L. P., Sherman, F., and Roder, H. (1997) Identification of the predominant non-native histidine ligand in unfolded cytochrome *c*. *Biochemistry 36*, 12535–12541.
5. Bhuyan, A. K., and Udgaonkar, J. B. (2001) Folding of horse cytochrome *c* in the reduced state. *J. Mol. Biol. 312*, 1135–1160.
6. Bhuyan, A. K., and Kumar, R. (2002) Kinetic barriers to the folding of horse cytochrome *c* in the reduced state. *Biochemistry 41*, 12821–12834.
7. Sosnick, T. R., Mayne, L., Hiller, R., and Englander, S. W. (1994) The barriers in protein folding. *Nat. Struct. Biol. 1*, 149–156.
8. Sosnick, T. R., Mayne, L., and Englander, S. W. (1996) Molecular collapse: the rate limiting step in two state cytochrome *c* folding. *Proteins 24*, 413–426.
9. Bhuyan, A. K. (2010) Off-pathway status for the alkali molten globule of horse ferricytochrome *c*, *Biochemistry* (DOI 10.1021/bi100880d).
10. Rao, D. K., Kumar, R., Yadaiah, M., and Bhuyan, A. K. (2006) The alkali molten globule state of ferrocytochrome *c*: extraordinary stability, persistent structure, and constrained overall dynamics. *Biochemistry 45*, 3412–3420.
11. Prabhu, N. P., Kumar, R., and Bhuyan, A. K. (2004) Folding barrier in horse cytochrome *c*: support for a classical folding pathway. *J. Mol. Biol. 337*, 195–208.
12. Bhuyan, A. K., Rao, D. K., and Prabhu, N. P. (2005) Protein folding in classical perspective: folding of horse cytochrome *c*. *Biochemistry 44*, 3034–3040.
13. Sosnick, T. R., Shtilerman, M. D., Mayne, L., and Englander, S. W. (1997) Ultrafast signals in protein folding and the polypeptide contracted state. *Proc. Natl. Acad. Sci. U.S.A. 94*, 8545–8550.
14. Roder, H., and Colón, W. (1997) Kinetic role of early intermediates in protein folding. *Curr. Opin. Struct. Biol. 7*, 15–28.
15. Shastry, M. C. R., and Roder, H. (1998) Evidence for barrier-limited protein folding kinetics on the microsecond time scale. *Nat. Struct. Biol. 5*, 385–392.
16. Qi, P. Q., Sosnick, T. R., and Englander, S. W. (1998) The burst phase in ribonuclease A folding: solvent dependence of the unfolded state. *Nat. Struct. Biol. 5*, 882–884.
17. Bhuyan, A. K., and Udgaonkar, J. B. (1999) Relevance of burst phase changes in optical signals of polypeptides during protein folding, in Perspectives in Structural Biology (Vijayan, M., et al. , Eds.) pp 293−303, University Press, Hyderabad, India.
18. Rao, D. K., Prabhu, N. P., and Bhuyan, A. K. (2006) Extensive misfolding in the refolding reaction of alkaline ferrocytochrome *c*. *Biochemistry 45*, 8393–8401.
19. Kuwajima, K., and Arai, M. (2000) The molten globule state: the physical and biological significance, in Mechanism of Protein Folding (Pain, R. H., Ed.) 2nd ed., pp 138−174, Oxford University Press, New York.
20. Arai, M., and Kuwajima, K. (2000) Role of the molten globule state in protein folding. *Adv. Protein Chem. 53*, 209–271.
21. Wolynes, P. G., Onuchic, J. N., and Thirumalai, D. (1995) Navigating the folding routes. *Science 267*, 1619–1620.
22. Colón, W., and Roder, H. (1996) Kinetic intermediates in the formation of the cytochrome *c* molten globule. *Nat. Struct. Biol. 3*, 1019–1025.
23. Mok, K. H., Nagashima, T., Day, I. J., Hore, P. J., and Dobson, C. M. (2005) Multiple subsets of side-chain packing in partially folded states of α-lactalbumins. *Proc. Natl. Acad. Sci. U.S.A. 102*, 8899–8904.
24. Nishimura, C., Dyson, H. J., and Wright, P. E. (2002) The apomyoglobin folding pathway revisited: structural heterogeneity in the kinetic burst phase intermediate. *J. Mol. Biol. 322*, 483–489.
25. Kumar, R., Prabhu, N. P., Rao, D. K., and Bhuyan, A. K. (2006) The alkali molten globule state of horse ferricytochrome *c*: observation of cold denaturation. *J. Mol. Biol. 364*, 483–495.
26. Nabuurs, S. M., Westphal, A. H., and van Mierlo, C. P. M. (2009) Noncooperative formation of the off-pathway molten globule during folding of the α-*β* parallel protein apoflavodoxin. *J. Am. Chem. Soc. 131*, 2739–2746.
27. Nabuurs, S. M., and van Mierlo, C, P. (2010) Interrupted hydrogen/deuterium exchange reveals the stable core of the remarkably helical molten globule of α-*β* parallel protein flavodoxin. *J. Biol. Chem. 285*, 4165–4172.
28. Moparthi, S. B., Fristedt, R., Mishra, R., Almstedt, K., Karlsson, M., Hammarström, P., and Carlsson, U. (2010) Chaperone activity of Cyp18 through hydrophobic condensation that enables rescue of transient misfolded molten globule intermediates. *Biochemistry 49*, 1137–1145.
29. Nishimura, C., Dyson, H. J., and Wright, P. E. (2006) Identification of native and non-native structure in kinetic folding intermediates of apomyoglobin. *J. Mol. Biol. 355*, 139–156.
30. Rösner, H. I., and Redfield, C. (2009) The human α-lactalbumin molten globule: comparison of structural preferences at pH 2 and pH 7. *J. Mol. Biol. 394*, 351–362.